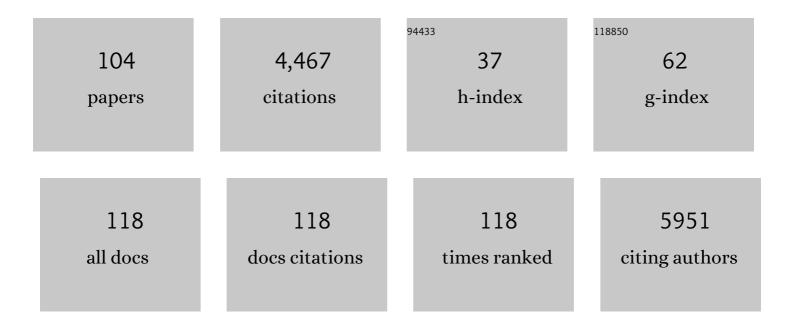
Shang-Te Danny Hsu

List of Publications by Year in descending order

Source: https://exaly.com/author-pdf/5856176/publications.pdf Version: 2024-02-01



SHANG-TE DANNY HELL

#	Article	IF	CITATIONS
1	Distinct shifts in site-specific glycosylation pattern of SARS-CoV-2 spike proteins associated with arising mutations in the D614G and Alpha variants. Glycobiology, 2022, 32, 60-72.	2.5	16
2	Sialic acid-containing glycolipids mediate binding and viral entry of SARS-CoV-2. Nature Chemical Biology, 2022, 18, 81-90.	8.0	141
3	The catalytic activity of TCPTP is auto-regulated by its intrinsically disordered tail and activated by Integrin alpha-1. Nature Communications, 2022, 13, 94.	12.8	16
4	BARD1 is an ATPase activating protein for OLA1. Biochimica Et Biophysica Acta - General Subjects, 2022, 1866, 130099.	2.4	1
5	Oxidation of catalytic cysteine of human deubiquitinase BAP1 triggers misfolding and aggregation in addition to functional loss. Biochemical and Biophysical Research Communications, 2022, 599, 57-62.	2.1	1
6	Impacts of Cancer-associated Mutations on the Structure–Activity Relationship of BAP1. Journal of Molecular Biology, 2022, 434, 167553.	4.2	4
7	Tumor suppressor BAP1 nuclear import is governed by transportin-1. Journal of Cell Biology, 2022, 221,	5.2	5
8	Direct Visualization of a 26 kDa Protein by Cryo-Electron Microscopy Aided by a Small Scaffold Protein. Biochemistry, 2021, 60, 1075-1079.	2.5	8
9	Cross-over Loop Cysteine C152 Acts as an Antioxidant to Maintain the Folding Stability and Deubiquitinase Activity of UCH-L1 Under Oxidative Stress. Journal of Molecular Biology, 2021, 433, 166879.	4.2	6
10	Tying up the Loose Ends: A Mathematically Knotted Protein. Frontiers in Chemistry, 2021, 9, 663241.	3.6	7
11	Converging experimental and computational views of the knotting mechanism of a small knotted protein. Biophysical Journal, 2021, 120, 2276-2286.	0.5	12
12	Structural polymorphism and substrate promiscuity of a ribosome-associated molecular chaperone. Magnetic Resonance, 2021, 2, 375-386.	1.9	1
13	Generation and Characterization of a Spike Glycoprotein Domain A-Specific Neutralizing Single-Chain Variable Fragment against Porcine Epidemic Diarrhea Virus. Vaccines, 2021, 9, 833.	4.4	4
14	Effect of SARS-CoV-2 B.1.1.7 mutations on spike protein structure and function. Nature Structural and Molecular Biology, 2021, 28, 731-739.	8.2	124
15	D614G mutation in the SARS-CoV-2 spike protein enhances viral fitness by desensitizing it to temperature-dependent denaturation. Journal of Biological Chemistry, 2021, 297, 101238.	3.4	46
16	Structure-guided antibody cocktail for prevention and treatment of COVID-19. PLoS Pathogens, 2021, 17, e1009704.	4.7	12
17	Targeting protein tyrosine phosphatase PTP-PEST (PTPN12) for therapeutic intervention in acute myocardial infarction. Cardiovascular Research, 2020, 116, 1032-1046.	3.8	13
18	Protein knots provide mechano-resilience to an AAA+ protease-mediated proteolysis with profound ATP energy expenses. Biochimica Et Biophysica Acta - Proteins and Proteomics, 2020, 1868, 140330.	2.3	10

#	Article	IF	CITATIONS
19	Cryo-EM analysis of a feline coronavirus spike protein reveals a unique structure and camouflaging glycans. Proceedings of the National Academy of Sciences of the United States of America, 2020, 117, 1438-1446.	7.1	94
20	Untying a Knotted SPOUT RNA Methyltransferase by Circular Permutation Results in a Domain-Swapped Dimer. Structure, 2019, 27, 1224-1233.e4.	3.3	18
21	Untying a Protein Knot by Circular Permutation. Journal of Molecular Biology, 2019, 431, 857-863.	4.2	18
22	A High-Throughput Interbacterial Competition Screen Identifies ClpAP in Enhancing Recipient Susceptibility to Type VI Secretion System-Mediated Attack by Agrobacterium tumefaciens. Frontiers in Microbiology, 2019, 10, 3077.	3.5	15
23	A Natively Monomeric Deubiquitinase UCH-L1 Forms Highly Dynamic but Defined Metastable Oligomeric Folding Intermediates. Journal of Physical Chemistry Letters, 2018, 9, 2433-2437.	4.6	13
24	Soluble Siglec-14 glycan-recognition protein is generated by alternative splicing and suppresses myeloid inflammatory responses. Journal of Biological Chemistry, 2018, 293, 19645-19658.	3.4	32
25	How Native and Non-Native Cations Bind and Modulate the Properties of GTP/ATP. Journal of Chemical Theory and Computation, 2018, 14, 3311-3320.	5.3	9
26	Comparative folding analyses of unknotted versus trefoil-knotted ornithine transcarbamylases suggest stabilizing effects of protein knots. Biochemical and Biophysical Research Communications, 2018, 503, 822-829.	2.1	14
27	Dissecting the Structure–Activity Relationship of Galectin–Ligand Interactions. International Journal of Molecular Sciences, 2018, 19, 392.	4.1	58
28	Topologically knotted deubiquitinases exhibit unprecedented mechanostability to withstand the proteolysis by an AAA+ protease. Scientific Reports, 2018, 8, 7076.	3.3	31
29	Entropic stabilization of a deubiquitinase provides conformational plasticity and slow unfolding kinetics beneficial for functioning on the proteasome. Scientific Reports, 2017, 7, 45174.	3.3	14
30	Lactose Binding Induces Opposing Dynamics Changes in Human Galectins Revealed by NMR-Based Hydrogen–Deuterium Exchange. Molecules, 2017, 22, 1357.	3.8	13
31	Familial Mutations and Post-translational Modifications of UCH-L1 in Parkinson's Disease and Neurodegenerative Disorders. Current Protein and Peptide Science, 2017, 18, 733-745.	1.4	25
32	Moenomycin Biosynthesis: Structure and Mechanism of Action of the Prenyltransferase MoeN5. Angewandte Chemie - International Edition, 2016, 55, 4716-4720.	13.8	19
33	Protein knotting through concatenation significantly reduces folding stability. Scientific Reports, 2016, 6, 39357.	3.3	5
34	Folding analysis of the most complex Stevedore's protein knot. Scientific Reports, 2016, 6, 31514.	3.3	32
35	The Knotted Protein UCH-L1 Exhibits Partially Unfolded Forms under Native Conditions that Share Common Structural Features with Its Kinetic Folding Intermediates. Journal of Molecular Biology, 2016, 428, 2507-2520.	4.2	44
36	Dual thio-digalactoside-binding modes of human galectins as the structural basis for the design of potent and selective inhibitors. Scientific Reports, 2016, 6, 29457.	3.3	70

#	Article	IF	CITATIONS
37	A novel transition pathway of ligand-induced topological conversion from hybrid forms to parallel forms of human telomeric G-quadruplexes. Nucleic Acids Research, 2016, 44, 3958-3968.	14.5	30
38	Interfacial Enzyme Function Visualized Using Neutron, X-Ray, and Light-Scattering Methods. , 2016, , 149-190.		1
39	NMR assignments of the peptidyl-prolyl cis–trans isomerase domain of trigger factor from E. coli. Biomolecular NMR Assignments, 2016, 10, 149-152.	0.8	3
40	A Multivalent Marine Lectin from <i>Crenomytilus grayanus</i> Possesses Anti-cancer Activity through Recognizing Globotriose Gb3. Journal of the American Chemical Society, 2016, 138, 4787-4795.	13.7	51
41	Structures of Trypanosome Vacuolar Soluble Pyrophosphatases: Antiparasitic Drug Targets. ACS Chemical Biology, 2016, 11, 1362-1371.	3.4	15
42	Comparative analysis of the folding dynamics and kinetics of an engineered knotted protein and its variants derived from HP0242 of <i>Helicobacter pylori</i> . Journal of Physics Condensed Matter, 2015, 27, 354106.	1.8	23
43	Site‧pecific Solid‧tate NMR Studies of "Trigger Factor―in Complex with the Large Ribosomal Subunitâ€50S. Angewandte Chemie - International Edition, 2015, 54, 4367-4369.	13.8	42
44	Unraveling the Folding Mechanism of the Smallest Knotted Protein, MJ0366. Journal of Physical Chemistry B, 2015, 119, 4359-4370.	2.6	44
45	Random-Coil Behavior of Chemically Denatured Topologically Knotted Proteins Revealed by Small-Angle X-ray Scattering. Journal of Physical Chemistry B, 2015, 119, 5437-5443.	2.6	20
46	Key Residues of Outer Membrane Protein Oprl Involved in Hexamer Formation and Bacterial Susceptibility to Cationic Antimicrobial Peptides. Antimicrobial Agents and Chemotherapy, 2015, 59, 6210-6222.	3.2	8
47	NMR assignments of the C-terminal domain of human galectin-8. Biomolecular NMR Assignments, 2015, 9, 427-430.	0.8	3
48	Conformational Transition of a Hairpin Structure to G-Quadruplex within the <i>WNT1</i> Gene Promoter. Journal of the American Chemical Society, 2015, 137, 210-218.	13.7	51
49	Solution structure and tandem DNA recognition of the C-terminal effector domain of PmrA from <i>Klebsiella pneumoniae</i> . Nucleic Acids Research, 2014, 42, 4080-4093.	14.5	24
50	Structural basis of sodium–potassium exchange of a human telomeric DNA quadruplex without topological conversion. Nucleic Acids Research, 2014, 42, 4723-4733.	14.5	52
51	Backbone NMR assignments of a topologically knotted protein in urea-denatured state. Biomolecular NMR Assignments, 2014, 8, 439-442.	0.8	10
52	NMR assignments of PI3-SH3 domain aided by protonless NMR spectroscopy. Biomolecular NMR Assignments, 2014, 8, 291-295.	0.8	0
53	NMR assignments of a hypothetical pseudo-knotted protein HP0242 from Helicobacter pylori. Biomolecular NMR Assignments, 2014, 8, 287-289.	0.8	2
54	Backbone NMR assignments of a topologically knotted protein in urea-denatured state. Biomolecular NMR Assignments, 2014, 8, 283-285.	0.8	11

#	Article	IF	CITATIONS
55	Nucleotide Contributions to the Structural Integrity and DNA Replication Initiation Activity of Noncoding Y RNA. Biochemistry, 2014, 53, 5848-5863.	2.5	17
56	Self-Assembly of MinE on the Membrane Underlies Formation of the MinE Ring to Sustain Function of the Escherichia coli Min System. Journal of Biological Chemistry, 2014, 289, 21252-21266.	3.4	18
57	Unfolding Kinetics of Human Telomeric G-Quadruplexes Studied by NMR Spectroscopy. Journal of Physical Chemistry B, 2014, 118, 931-936.	2.6	11
58	Structure, function and inhibition of ent-kaurene synthase from Bradyrhizobium japonicum. Scientific Reports, 2014, 4, 6214.	3.3	44
59	A Nanobody Binding to Non-Amyloidogenic Regions of the Protein Human Lysozyme Enhances Partial Unfolding but Inhibits Amyloid Fibril Formation. Journal of Physical Chemistry B, 2013, 117, 13245-13258.	2.6	42
60	Crystal Structure of Vaccinia Viral A27 Protein Reveals a Novel Structure Critical for Its Function and Complex Formation with A26 Protein. PLoS Pathogens, 2013, 9, e1003563.	4.7	32
61	Residue-Specific Annotation of Disorder-to-Order Transition and Cathepsin Inhibition of a Propeptide-Like Crammer from D. melanogaster. PLoS ONE, 2013, 8, e54187.	2.5	0
62	A molten globule-to-ordered structure transition of <i>Drosophila melanogaster</i> crammer is required for its ability to inhibit cathepsin. Biochemical Journal, 2012, 442, 563-572.	3.7	8
63	Functional Dynamics of Proteins. Computational and Mathematical Methods in Medicine, 2012, 2012, 1-3.	1.3	1
64	1H, 13C and 15N resonance assignments of human muscle acylphosphatase. Biomolecular NMR Assignments, 2012, 6, 27-29.	0.8	16
65	The Effect of Parkinson's-Disease-Associated Mutations on the Deubiquitinating Enzyme UCH-L1. Journal of Molecular Biology, 2011, 407, 261-272.	4.2	61
66	Experimental free energy surfaces reveal the mechanisms of maintenance of protein solubility. Proceedings of the National Academy of Sciences of the United States of America, 2011, 108, 21057-21062.	7.1	65
67	Backbone assignments of the 26ÂkDa neuron-specific ubiquitin carboxyl-terminal hydrolase L1 (UCH-L1). Biomolecular NMR Assignments, 2010, 4, 41-43.	0.8	9
68	Folding Study of Venus Reveals a Strong Ion Dependence of Its Yellow Fluorescence under Mildly Acidic Conditions. Journal of Biological Chemistry, 2010, 285, 4859-4869.	3.4	19
69	Transient Tertiary Structure Formation within the Ribosome Exit Port. Journal of the American Chemical Society, 2010, 132, 16928-16937.	13.7	69
70	Local Cooperativity in an Amyloidogenic State of Human Lysozyme Observed at Atomic Resolution. Journal of the American Chemical Society, 2010, 132, 15580-15588.	13.7	55
71	Towards Multiparametric Fluorescent Imaging of Amyloid Formation: Studies of a YFP Model of α-Synuclein Aggregation. Journal of Molecular Biology, 2010, 395, 627-642.	4.2	72
72	Structure and Properties of a Complex of α-Synuclein and a Single-Domain Camelid Antibody. Journal of Molecular Biology, 2010, 402, 326-343.	4.2	164

#	Article	IF	CITATIONS
73	Small molecule-mediated inhibition of translation by targeting a native RNA G-quadruplex. Organic and Biomolecular Chemistry, 2010, 8, 2771.	2.8	101
74	Probing ribosome-nascent chain complexes produced in vivo by NMR spectroscopy. Proceedings of the National Academy of Sciences of the United States of America, 2009, 106, 22239-22244.	7.1	81
75	1H, 15N and 13C assignments of the dimeric ribosome binding domain of trigger factor from Escherichia coli. Biomolecular NMR Assignments, 2009, 3, 17-20.	0.8	12
76	1H, 15N and 13C assignments of domain 5 of DictyosteliumÂdiscoideum gelation factor (ABP-120) in its native and 8M urea-denatured states. Biomolecular NMR Assignments, 2009, 3, 29-31.	0.8	18
77	1H, 15N and 13C assignments of yellow fluorescent protein (YFP) Venus. Biomolecular NMR Assignments, 2009, 3, 67-72.	0.8	15
78	1H, 13C and 15N assignments of a camelid nanobody directed against human α-synuclein. Biomolecular NMR Assignments, 2009, 3, 231-233.	0.8	29
79	Chaperone proteostasis in Parkinson's disease: stabilization of the Hsp70/α-synuclein complex by Hip. EMBO Journal, 2009, 28, 3758-3770.	7.8	110
80	A G-Rich Sequence within the <i>c-kit</i> Oncogene Promoter Forms a Parallel G-Quadruplex Having Asymmetric G-Tetrad Dynamics. Journal of the American Chemical Society, 2009, 131, 13399-13409.	13.7	195
81	Accurate Random Coil Chemical Shifts from an Analysis of Loop Regions in Native States of Proteins. Journal of the American Chemical Society, 2009, 131, 16332-16333.	13.7	85
82	Probing Side-Chain Dynamics of a Ribosome-Bound Nascent Chain Using Methyl NMR Spectroscopy. Journal of the American Chemical Society, 2009, 131, 8366-8367.	13.7	37
83	Use of Protonless NMR Spectroscopy To Alleviate the Loss of Information Resulting from Exchange-Broadening. Journal of the American Chemical Society, 2009, 131, 7222-7223.	13.7	69
84	Structure, Dynamics and Folding of an Immunoglobulin Domain of the Gelation Factor (ABP-120) from Dictyostelium discoideum. Journal of Molecular Biology, 2009, 388, 865-879.	4.2	32
85	The folding, stability and conformational dynamics of β-barrel fluorescent proteins. Chemical Society Reviews, 2009, 38, 2951.	38.1	72
86	A Small Molecule That Disrupts G-Quadruplex DNA Structure and Enhances Gene Expression. Journal of the American Chemical Society, 2009, 131, 12628-12633.	13.7	123
87	A Nonpeptidic Reverse Turn that Promotes Parallel Sheet Structure Stabilized by CHâ‹â‹O Hydrogen Bonds in a Cyclopropane γâ€Peptide. Angewandte Chemie - International Edition, 2008, 47, 7099-7102.	13.8	45
88	Diarylethynyl Amides That Recognize the Parallel Conformation of Genomic Promoter DNA G-Quadruplexes. Journal of the American Chemical Society, 2008, 130, 15950-15956.	13.7	151
89	Evolution Rescues Folding of Human Immunodeficiency Virus-1 Envelope Glycoprotein GP120 Lacking a Conserved Disulfide Bond. Molecular Biology of the Cell, 2008, 19, 4707-4716.	2.1	12
90	The extremely slowâ€exchanging core and acidâ€denatured state of green fluorescent protein. HFSP Journal, 2008, 2, 378-387.	2.5	17

#	Article	IF	CITATIONS
91	Structure and dynamics of a ribosome-bound nascent chain by NMR spectroscopy. Proceedings of the National Academy of Sciences of the United States of America, 2007, 104, 16516-16521.	7.1	116
92	Structural Motifs of Lipid II-Binding Lantibiotics as a Blueprint for Novel Antibiotics. Anti-Infective Agents in Medicinal Chemistry, 2006, 5, 245-254.	0.6	5
93	The Solution Structure of the AppA BLUF Domain: Insight into the Mechanism of Light-Induced Signaling. ChemBioChem, 2006, 7, 187-193.	2.6	111
94	Characterization and Structural Analyses of Nonspecific Lipid Transfer Protein 1 from Mung Bean. Biochemistry, 2005, 44, 11646-11646.	2.5	0
95	Isolation and structural characterization of epilancin 15X, a novel lantibiotic from a clinical strain of Staphylococcus epidermidis. FEBS Letters, 2005, 579, 1917-1922.	2.8	71
96	Entropy Calculation of HIV-1 Env gp120, its Receptor CD4, and their Complex: An Analysis of Configurational Entropy Changes upon Complexation. Biophysical Journal, 2005, 88, 15-24.	0.5	60
97	Characterization and Structural Analyses of Nonspecific Lipid Transfer Protein 1 from Mung Beanâ€,‡. Biochemistry, 2005, 44, 5703-5712.	2.5	56
98	Atomic insight into the CD4 binding-induced conformational changes in HIV-1 gp120. Proteins: Structure, Function and Bioinformatics, 2004, 55, 582-593.	2.6	39
99	The nisin–lipid II complex reveals a pyrophosphate cage that provides a blueprint for novel antibiotics. Nature Structural and Molecular Biology, 2004, 11, 963-967.	8.2	505
100	NMR Study of Mersacidin and Lipid II Interaction in Dodecylphosphocholine Micelles. Journal of Biological Chemistry, 2003, 278, 13110-13117.	3.4	113
101	Mapping the Targeted Membrane Pore Formation Mechanism by Solution NMR:Â The Nisin Z and Lipid II Interaction in SDS Micelles. Biochemistry, 2002, 41, 7670-7676.	2.5	68
102	The solution structure of [d(CGC)r(amamam)d(TTTGCG)]2. Journal of Biomolecular NMR, 2001, 21, 209-220.	2.8	3
103	The solution structure of [d(CGC)r(aaa)d(TTTGCG)]2: hybrid junctions flanked by DNA duplexes. Nucleic Acids Research, 2000, 28, 1322-1331.	14.5	9
104	Hydration of [d(CGC)r(aaa)d(TTTGCG)]2. Journal of Molecular Biology, 2000, 295, 1129-1137.	4.2	6